Semnan University

Progress in Physics of Applied Materials

journal homepage: https://ppam.semnan.ac.ir/

Electrochemically grown superparamagnetic Co-Fe_3O_4 nanoparticles onto functionalized graphene oxide for biomedical aims

Mustafa Aghazadeh[a,*], Isa Karimzadeh[b]

[a]*Nuclear Fuel Cycle Research School, Nuclear Science and Technology Research Institute (NSTRI), Tehran, Iran*
[b]*Department of Physics, Faculty of Science, Central Tehran Branch, Islamic Azad University, Tehran, Iran*

ARTICLE INFO

Article history:
Received: 10 December 2023
Revised: 31 January 2024
Accepted: 3 February 2024

Keywords:
Bare Co-Fe_3O_4
Co^{2+}-doping
Graphene Oxide
Nanocomposite

ABSTRACT

Herein, we report the structural, morphological, and chemical properties of the electrochemically grown Co^{2+}-doped magnetite (Co-Fe_3O_4) nanoparticles onto functionalized graphene oxide layers (Co^{2+}-doped iron oxide@f-GO composite). The deposition process is done at the galvanostatic mode in the two-electrode system by applying the constant current density of 5 mA cm^{-2}. The fabricated Co^{2+}-doped iron oxide@f-GO composite is characterized via Scanning Electron Microscopy, energy dispersive X-ray analysis, Fourier Transform Infrared Spectroscopy (FTIR), Transmission Electron Microscopy (TEM), and X-Ray diffraction analysis. TEM observation revealed that Co-Fe_3O_4 has fine particle morphology with size of 5-10 nm. The FTIR data proved the graphene-based chemical nature of the fabricated composite. The superparamagnetic nature of the prepared composite is proved by vibrating sample magnetometer tests, which verified that the prepared metal-cation doped Fe_3O_4 nanoparticles grown onto functionalized GO layers could be an interesting candidate for further manipulations for biomedical aims such as drug delivery, magnetic resonance imaging, and hyperthermia.

1. Introduction

Many applications benefit from the physico-chemical characteristics of superparamagnetic iron oxide (SPIO). Many of these uses focus on the use of SPIO for theragnostic and diagnostic aims. The superparamagnetic abilities of SPIOs provide their suitable performances in MRI, magnetic hyperthermia, and targeted drug delivery applications [1]. The incorporation of SPIO into a drug carrier and/or modifications on their surfaces enable them to be targeted to many different tumor tissues such as brain cancer, breast cancer, prostate cancer, and bone cancer [2]. The using SPIO in biological applications may ~~has~~ have major drawback such as its instability and tendency to form aggregates via interaction in aqueous environments (i.e. van der Waals interaction) causing their incompatibility with physiological mediums [3]. Doping of SPIO by some suitable cations may favor magnetic dipolar interactions between particles, where these interactions may change SPIOs intrinsic magnetic characters [4]. Also, the formation of bigger aggregates may increase the risk of recognition by the reticuloendothelial system (RES) [5].

It is well known that thermal treatment of as-prepared spinel ferrite nanoparticles at high temperatures can reduce the surface disorder and improve the magnetic properties, but this leads to significant grain growth [6,7]. Several papers were devoted to studying the changes of the physical-chemical and especially magnetic properties of spinel ferrite nanoparticles through effects of method of synthesis, which are associated with phase and size changes during thermal treatment [8,9]. On the other hand, compositing spinel ferrites with graphene oxide and doping with metal cations can modify their magnetic characteristics by directly affecting the magnetic anisotropy constant [10-12]. For example, doped Co^{2+} ions in Fe_3O_4 are in a charge state of 2 + and substitute the Fe^{2+} in the B site of Fe_3O_4. All

* Corresponding author.
E-mail address: maghazadeh@aeoi.org.ir

Cite this article as:
Aghazadeh, M., Karimzadeh, I., 2023. Electrochemically grown superparamagnetic Co-Fe_3O_4 nanoparticles onto functionalized graphene oxide for biomedical aims. *Progress in Physics of Applied Materials*, 4(1), pp.1-6. DOI: 10.22075/PPAM.2024.32630.1076

the films exhibit room temperature ferromagnetism. Co^{2+} doping changes the coercivity and reduces saturation magnetization. The density of states near the Fermi level is reduced by Co^{2+} doping due to the decrease of Fe^{2+} in the B site, which might responsible for the decrease in conductivity and magnetoresistance of Co-doped Fe_3O_4 [12,13]. Therefore, many studies have been focused on increasing the bioavailability and biodistribution of SPIOs by proper structural and surface modifications as well as composition with graphene materials, which enhance their magnetization and stability without losing their natural properties. Metal-ion doping the surface of SPIO with a biocompatible polymer is one of the most common ways to achieve this purpose. The usual synthetic routes for SPIOs vary from physical to chemical methods. Nevertheless, there are also a few studies showing that they can be synthesized by electrochemical route [14].

In this paper, we report Co^{2+}-doped magnetite (Co-Fe_3O_4) nanoparticles onto functionalized graphene oxide layers (Co^{2+}-doped iron oxide@f-GO composite) through cathodic deposition route. The morphological, structural, and magnetic characteristics of the obtained Co^{2+}-doped iron oxide@f-GO composite were respectively investigated through different techniques of SEM, XRD, FT-IR, and VSM.

2. Experimental

2.1. Starting Materials

For preparation of deposition bath, the following chemical compounds were used:

(*i*) Cobalt nitrate hexahydrate [Merck, $Co(NO_3)_2.6H_2O$, 99.99%],

(*ii*) Iron (II) chloride tetrahydrate (Merck, $FeCl_2{\cdot}4H_2O$, 99%],

(*iii*) Iron (III) nitrate nonahydrate [Merck, $Fe(NO_3)_3.9H_2O$, 99.9%]

(*iv*) functionalized graphene oxide [f-GO, from IRRIP company].

2.2. Composite preparation

Electro-chemical synthesis from an aqueous solution containing dispersed functionalized GO was used to prepare composite. The electrochemical cell was 200 *ml* beaker, where two stainless steel (SS321) plates were put parallel in it. Then, 100 *ml* bath deposition was prepared as follow: 5*mg* f-GO powder was first added into deionized H_2O and sonicated for 6h; purchased salts (i.e. 5*mg* $FeCl_2{\cdot}4H_2O$, 30*mg* $Fe(NO_3)_3.9H_2O$, and 2*mg* $Co(NO_3)_2.6H_2O$) were then added into the dispersed f-GO powder solution and stirred at 25 °C for 12h. The Electro-chemical syntheses were run in the current density of 5 mA cm^{-2} for 25 min. At the end of each run, the black thin film deposited onto SS321 was removed from the steel surface. The obtained powder was dried at 100 °C for 2h. After that, the obtained black powder named as Co^{2+}-doped iron oxide@f-GO composite.

2.3. Composite characterization

The magnetic data and the magnetization hysteresis curve for the prepared Co^{2+}-doped iron oxide@f-GO composite were obtained through vibrating sample magnetometer (VSM, Model: Lake Shore 7400). The crystal structure of sample was determined by powder X-ray diffraction (XRD, a Phillips PW-1800 diffractometer with Co Kα radiation (λ=1.789 Å)). Morphological images of the prepared Co^{2+}-doped iron oxide@f-GO composite were provided by scanning electron microscopy instrument (SEM, Model ZEISS with accelerating voltage of 100 kV). The FT-IR spectrum of the fabricated composite was recorded by a Bruker Vector 22 Fourier transformed infrared spectroscope.

3. Results and discussion

SEM images and elemental analysis of the fabricated Co^{2+}-doped iron oxide@f-GO composite are shown in Figure 1. For the fabricated composite, two types of morphologies are observed in Figs. (1a and b) which included particle morphology related to the Co-Fe_3O_4 and the layered morphology due to the f-GO content of the fabricated Co^{2+}-doped iron oxide@f-GO composite.

The EDS data of the composite is demonstrated in Figs. 1c and d. As seen in Fig. 1c, this sample includes the carbon content in its composition revealing the graphene content of the Co-doped iron oxide@f-GO composite. As seen in Table presented as Fig. 1d, the composite powder has elemental weight percentages of 13.46% carbon and 9.83 % Co, 16.67 % O, and 59.92 %Fe. This data is comparable with those reported in Ref. [15] for Co^{2+}-doped iron oxide (i.e. 65.25 wt% iron, 9.85 wt% Cobalt, and 26.90 wt% Oxygen). Hence, the iron oxide core of the fabricated composite is confirmed through the presence of Fe and O elements in Fig. 1c. The cobalt presence (i.e. 9.83%) supports its cations doping into Fe_3O_4 structure during the synthesis. Also, the f-GO presence within the composite product, which has been resulted from the 13.46% C content of the final composite.

TEM image presented in Fig. 1e revealed that Co-Fe_3O_4 has fine particle morphology with size of 5-10 nm. Furthermore, the plate-like morphology is also observed for the graphene oxide (GO), where Co-Fe_3O_4 particles have been deposited onto these plates (Fig. 1e). These evidences clearly verified the fabrication of the Co-Fe_3O_4 nanoparticles deposited onto carboxylic-functionalized GO composite through our simple applied electrochemical strategy.

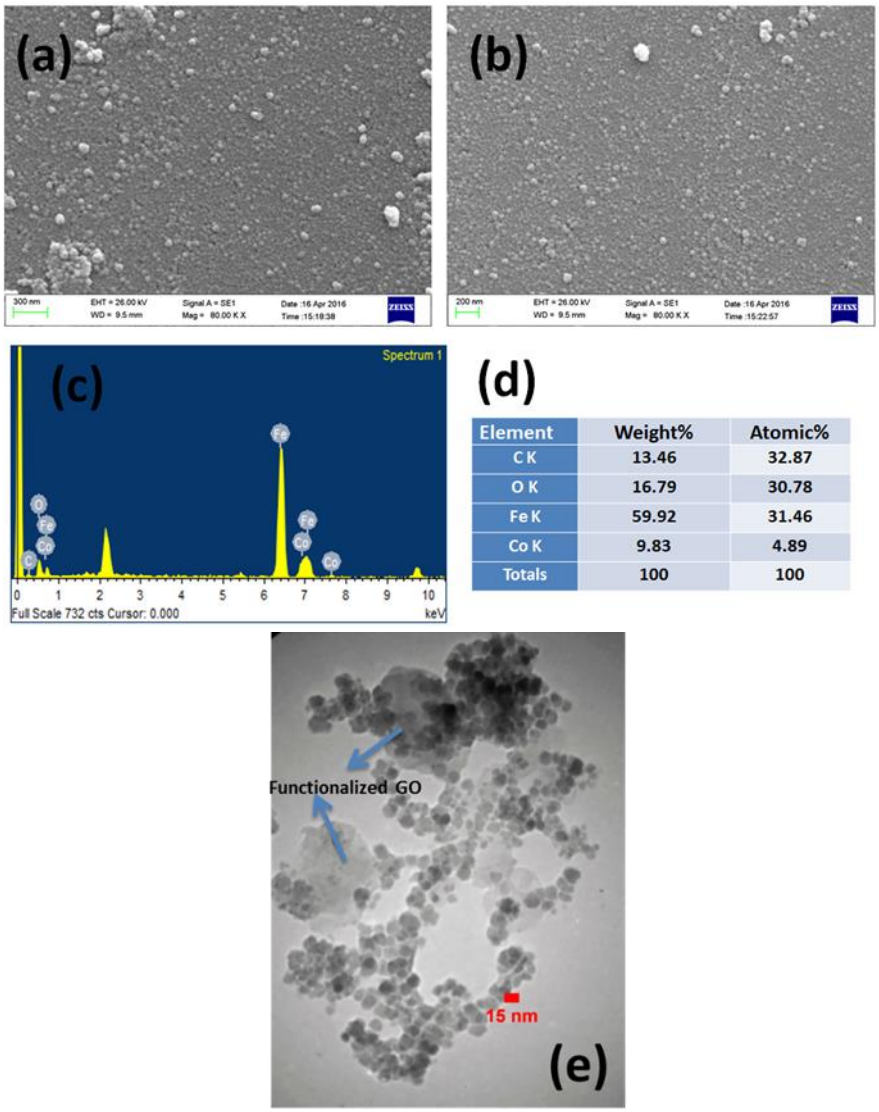

Fig. 1. (a,b) SEM images, (c,d) EDS, and (e)TEM image of the synthesized Co-Fe_3O_4 deposited onto functionalized GO.

FT-IR spectrum of the Co-Fe_3O_4 particles deposited onto carboxylic-functionalized GO is shown in Fig. 2. The IR bands below 700 cm^{-1} is due to the metal-oxygen vibration bands [16,17]. There are two distinct bands at 571-575 cm^{-1} and 442-447 cm^{-1}, which are related to the Fe-O-Fe and/or Fe-O-Co vibrations [16,17]. Also, for both samples, the broad band at 3400-3450 cm^{-1} is related to the vibration mode of OH groups attached onto the Co^{2+}doped Fe_3O_4 [17] and the absorption peaks at 1629-1632 cm^{-1} is originated from the stretching vibration of water molecules linked into the Fe_3O_4 surface [16]. Notably, IR peaks of the nitrate and carbonate ions are observed at 1510, 1379, and 1272 cm^{-1} [16,17]. The abortions at the wavenumbers of 950-1300 cm^{-1}, 1400-1550 cm^{-1}, and 2800-2950 cm^{-1} are related to the graphene part of the fabricated composite. The absorption band at about 1540 cm^{-1} is clearly due to the skeletal vibration of the graphene layers [18]. Furthermore, the C-O-C at 1122 cm^{-1} [18], C-H bending vibrations at 1341 cm^{-1} and 1384 cm^{-1} [19], C-H stretching at 2854 cm^{-1} and 2920 cm^{-1} [20], C=C stretching at 1625 cm^{-1} [20], and C-O-H stretching at 1453 cm^{-1} and 3436 cm^{-1} [22,23] are observed. The IR results proved the graphene-based chemical nature of the fabricated composite.

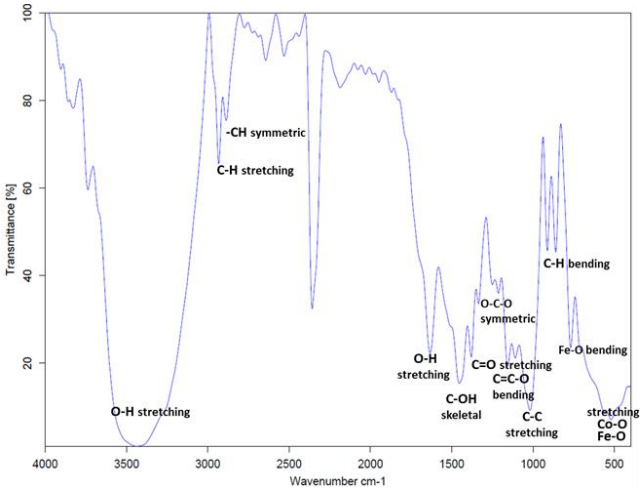

Fig. 2. FT-IR spectrum of the Co-Fe_3O_4 deposited onto carboxylic-functionalized GO.

XRD pattern of the fabricated composite is given in Fig. 3. In this pattern, several XRD diffractions are observed at 2tetha of 19.26°, 28.89°, 32.55°, 42.45°, 53.77°, 56.22°,

62.94 °, and 74.13°, which are related to the miller indices of (111), (220), (311), (400), (422), (511), (440), and (622). The XRD pattern of the prepared composite is completely matched with those of magnetite phase of Fe_3O_4 (JCPDS number of 01-088-0315) [17,20]. This finding supported that Co^{2+}-doped iron oxide has spinel crystal structure with the cubic $Fd\bar{3}m$ space group. In this structure, Fe^{2+} is bonded to four equivalent O^{2-} atoms to form FeO_4 tetrahedra that share corners with twelve equivalent FeO_6 octahedra. Notably, some of the Fe^{2+} cations have been replaced by doped Co^{2+} cation in the tetrahedral position [15,16]. Hence, the XRD pattern of the composite has no change with cobalt doping into the magnetite crystal structure. Also, there is a diffraction peak at $2\theta=13.5^o$, which is due to the graphene oxide [20,21]. Hence, the fabrication of cobalt cations doped Co^{2+}-doped Fe_3O_4@f-GO composite is verified through this XRD pattern. It should be noted that Co^{2+} doping into the Fe_3O_4 in the presence of graphene layers has no change in its crystal structure. The average crystallite size (D) was calculated from the diffraction line-width of XRD patterns, based on Scherrer's relation ($D=0.9\lambda/\beta \cos(\theta)$), where, β is the full width at half maxima (FWHM) of the (311) peak. The average crystalline size of 4.7 nm was calculated for the Co^{2+}-doped Fe_3O_4 particles.

The Magnetization curve and the extracted magnetic data for the fabricated sample was provided using vibrating sample magnetometer (VSM) analysis via recording magnetization *vs.* applied field in the range of -2000 to 2000 Oe. The VSM profile of sample is shown in Fig. 4. From this curve, some magnetic parameters of sample including saturation magnetization (*Ms*), remnant magnetization (*Mr*), and coercivity (*Hci*) are obtained which are listed in Table 1. The M-H profile of the fabricated composite has superparamagnetic nature. As listed in Table 1, the values of *Ms*, *Mr,* and *Hci* for the Co-Fe_3O_4@f-GO composite were obtained to be 55.67 emu g^{-1}, 1.47 emu g^{-1}, and 41.12 G, respectively (Table 1). These values confirmed the superparamagnetic character of the Co-Fe_3O_4@f-GO composite. As compared with the pure Co-Fe_3O_4 sample [15], the composite exhibited the high saturation magnetization (*Ms*) revealing its better superparamagnetic properties. This observation reveals that the saturation magnetization of Co^{2+}-doped Fe_3O_4 particles is improved by compositing with graphene. In fact, with the deposition of Co^{2+}-doped Fe_3O_4 particles onto the functionalized graphene oxide plates/layers, their magnetic parameters are modified as compared with pure Co^{2+}-doped Fe_3O_4 particles. This modification is due to the batter particle morphology (i.e. not agglomerated form) of the Fe_3O_4 particles in the composite sample (Fig. 1d). In fact, the f-GO layers prevent Co^{2+}-doped Fe_3O_4 particles to stack each other as well as agglomeration. The other magnetic data of the fabricated composite (i.e. positive *Hci*, negative *Hci*, negative *Mr,* and positive *Mr*) are comparable with those of the bare Co-Fe_3O_4 particles (as seen in Table 1).

Table 1. Magnetization characteristics of bare Co-Fe_3O_4 nanoparticles and Co-Fe_3O_4@f-GO composite.

Sample name	*Ms* (emu/g)	Coercivity (G)	Positive *Hci* (G)	Negative *Hci* (G)	Negative *Mr*	Positive *Mr*	Retentivity *Mr* (emu/g)	Refs.
Bare Co-Fe_3O_4	52.14	44.46	36.44	-52.48	-1.41	2.05	1.73	[15]
Co-Fe_3O_4@f-GO	55.67	41.12	34.64	-47.61	-1.25	1.69	1.47	This work

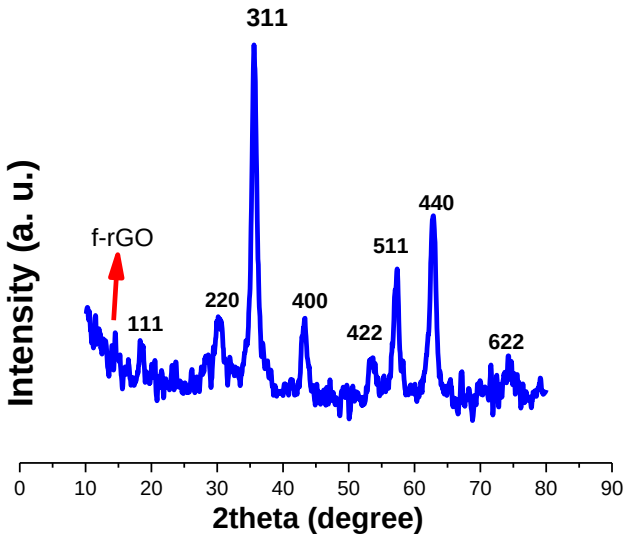

Fig. 3. XRD pattern of the prepared Co^{2+}-doped iron oxide@f-GO composite.

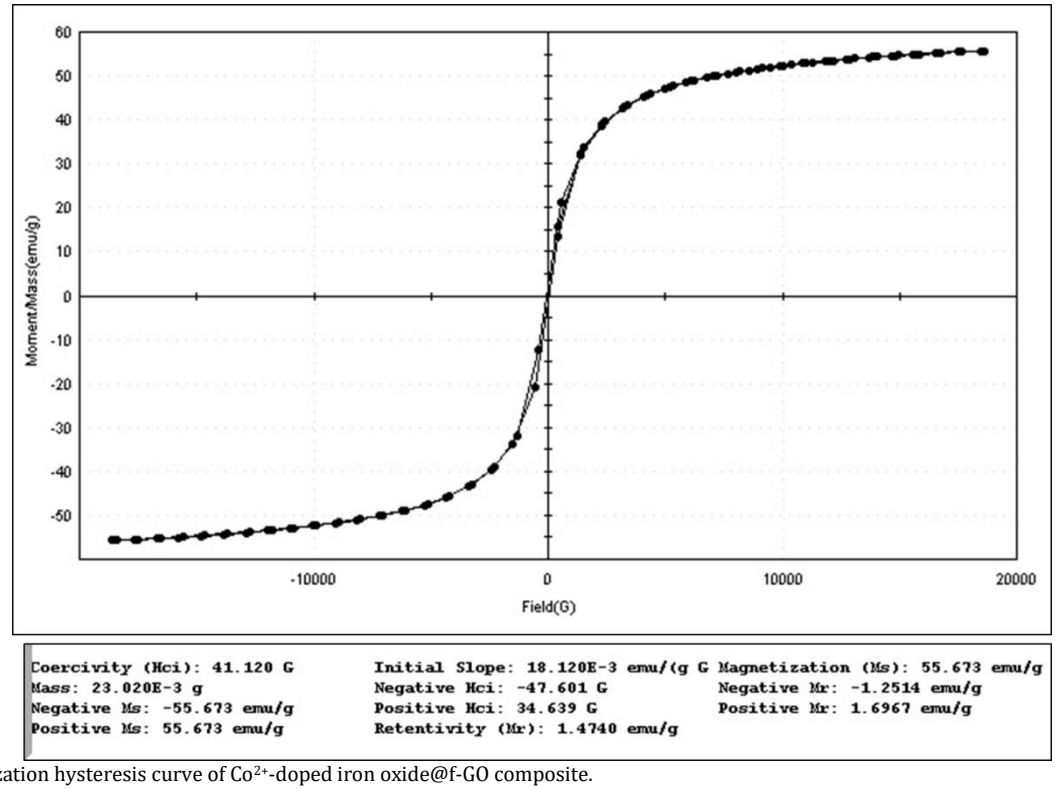

Fig. 4. Magnetization hysteresis curve of Co^{2+}-doped iron oxide@f-GO composite.

4. Conclusion

An electrochemical method was applied for the deposition of Co-Fe_3O_4 particles onto functionalized graphene oxide layers to obtain Co-Fe_3O_4@f-GO composite. The results of the SEM, TEM, and EDAX analyses showed 9.83% Co^{2+} cations into Fe_3O_4 structure during the synthesis and a mean size of 5 nm for the obtained Co-Fe_3O_4 particles. The composite exhibited magnetic parameters of *Ms*=55.67 emu g^{-1}, *Mr*=1.47 emu g^{-1}, and *Hci*=41.42 G, which verified its superparamagnetic nature. An improvement in magnetic nature of Fe_3O_4 particles was observed by their doping with Co^{2+} cations and compositing with functionalized graphene oxide.

Acknowledgements

There is nothing to acknowledgement.

Conflicts of Interest

The author declares that there is no conflict of interest regarding the publication of this article.

References

[1] Kermanian, M., Sadighian, S., Ramazani, A., Naghibi, M., Khoshkam, M. and Ghezelbash, P. 2021. Inulin-Coated Iron Oxide Nanoparticles: A Theranostic Platform for Contrast-Enhanced MR Imaging of Acute Hepatic Failure. *ACS Biomaterials Science and Engineering*, *7*(6), pp. 2701-2715.

[2] Senturk, F., Cakmak, S., Kocum, I. C., Gumusderelioglu, M. and Ozturk, G.G. 2021. GRGDS-conjugated and curcumin-loaded magnetic polymeric nanoparticles for the hyperthermia treatment of glioblastoma cells. *Colloids and Surfaces A: Physicochemical and Engineering Aspects*, *622*, p. 126648.

[3] Halevas, E., Mavroidi, B., Nday, C.M., Tang, J., Smith, G.C., Boukos, N., Litsardakis, G., Pelecanou, M. and Salifoglou, A. 2020. Modified magnetic core-shell mesoporous silica nano-formulations with encapsulated quercetin exhibit anti-amyloid and antioxidant activity. *Journal of Inorganic Biochemistry*, *213*, p. 111271.

[4] Aghazadeh, M., Karimzadeh, I., Ghannadi Maragheh, M., Ganajli, M.R. 2018. Gd^{3+} doped Fe_3O_4 nanoparticles with proper magnetic and supercapacitive characteristics: A novel synthesis platform and characterization. *Korean Journal of Chemical Engin*eering, *35*, pp. 1341-1347.

[5] Pucci, C., Degl'Innocenti, A., Belenli Gümüş, M. and Ciofani, G. 2022. Superparamagnetic iron oxide nanoparticles for magnetic hyperthermia: recent advancements, molecular effects, and future directions in the omics era. *Biomaterials Science*, *10*, pp. 2103-2121.

[6] Gholizadeh, A. and Jafari, E. 2017. Effects of sintering atmosphere and temperature on structural and magnetic properties of Ni-Cu-Zn ferrite nano-particles: Magnetic enhancement by a reducing atmosphere. *Journal of Magnetism and Magnetic Materials*, *422*, pp. 328-336.

[7] Gholizadeh, A. 2018. A comparative study of the physical properties of Cu-Zn ferrites annealed under different atmospheres and temperatures: Magnetic enhancement of $Cu_{0.5}Zn_{0.5}Fe_2O_4$ nanoparticles by a reducing atmosphere. *Journal of Magnetism and Magnetic Materials*, *452*, pp. 389-397.

[8] Gholizadeh, A. 2017. A comparative study of physical properties in Fe_3O_4 nanoparticles prepared by coprecipitation and citrate methods. *Journal of the American Ceramic Society*, *100* (8), pp. 3577-3588.

[9] Mojahed, M., Rezagholipour Dizaji, H. and Gholizadeh, A. 2022. Structural, magnetic, and dielectric properties of

Ni/Zn co-substituted $CuFe_2O_4$ nanoparticles. *Physica B: Condensed Matter*, *646*, p. 414337.

[10] Abharya, A. and Gholizadeh, A. 2020. Structural, Optical and Magnetic Feature of Core-Shell Nanostructured Fe_3O_4@GO in Photocatalytic Activity." *Iranian Journal of Chemistry and Chemical Engineering*, *39* (2), pp. 49-58.

[11] Deka, B., Cho, J., Lee, Y.-W., Yoo, I.-R., Ahn, C.W. and Cho, K.-H. 2021. Cation distribution and magnetostrictive strain in $CuFe_{2-x}Ga_xO_4$ ceramics. *Ceramic International*, *47*(9) pp. 11848-11855.

[12] Ran, F.Y., Tsunemaru, Y., Hasegawa, T., Takeichi, Y., Harasawa, A., Yaji, K. Kim, S. and Kakizaki, A., 2011. Valence band structure and magnetic properties of Co-doped Fe_3O_4(100) films. *Journal of Applied Physics*, *109* (12), p. 123919.

[13] Choupani, M. and Gholizadeh, A. 2023. Correlation between structural phase transition and physical properties of Co^{2+}/Gd^{3+} co-substituted copper ferrite. *Journal of Rare Earths*, In press, https://doi.org/10.1016/j.jre.2023.06.011.

[14] Aghazadeh, M., Karimzadeh, I., Ganjali, M.R. and Behzad, A. 2017. Mn^{2+}-doped Fe_3O_4 nanoparticles: a novel preparation method, structural, magnetic and electrochemical characterizations. *Journal of Materials Science: Materials in Electronics*, *28*, pp. 18121–18129

[15] Aghazadeh, M. and Ganjali, M.R. 2018. One-pot electrochemical synthesis and assessment of super-capacitive and super-paramagnetic performances of Co^{2+} doped Fe_3O_4 ultra-fine particles. *Journal of Materials Science: Materials in Electronics*, *29*, pp. 2291-2300.

[16] Aghazadeh, M., Forati-Rad, H., Yavari, K. and Mohammadzadeh, K. 2021. On-pot fabrication of binder-free composite of iron oxide grown onto porous N-doped graphene layers with outstanding charge storage performance for supercapacitors. *Journal of Materials Science: Materials in Electronics*, *32*, pp. 13156-13176.

[17] Malek Barmi, A., Moosavian, M.A., Aghazadeh, M. and Golikand, A.N. 2020. One-pot EPD/ECD fabrication of high-performance binder-free nanocomposite based on the Fe_3O_4 nanoparticles/porous graphene sheets for supercapacitor applications. *Journal of Materials Science: Materials in Electronics*, *31*, pp. 19569-19586.

[18] Dehghanzad, B., Razavi, Aghjeh M. K., Rafeie, O., Tavakoli, A. and Oskooi, A.J. 2016. Synthesis and characterization of graphene and functionalized graphene via chemical and thermal treatment methods. *RSC Advances*, *6*, pp. 3578-3585.

[19] Aziz, M., Abdul Halima, F. S. and Jaafar, J. 2014. Preparation and Characterization of Graphene Membrane Electrode Assembly. *Jurnal Teknologi*, *69*(9), pp. 11-24.

[20] Naebe, M., Wang, J., Amini, A., Khayyam, H., Hameed, N., Li, L.H., Chen, Y. and Fox, B. 2014. Mechanical Property and Structure of Covalent Functionalised Graphene/Epoxy Nanocomposites. *Scientific Reports*, *4*, p. 4375.

[21] Wang, H., Wei, C., Zhu, K., Zhang, Y., Gong, C., Guo, J., Zhang, J., Yu, L. and Zhang, J. 2017. Transparent and Self-Supporting Graphene Films with Wrinkled- Graphene-Wall-Assembled Opening Polyhedron Building Blocks for High Performance Flexible/Transparent Supercapacitors. *ACS Applied Materials and Interfaces*, *9*(11), pp. 9763-9771.